Available online at www.sciencedirect.com

ScienceDirect

www.elsevier.com/locate/jes

JES JOURNAL OF ENVIRONMENTAL SCIENCES

www.jesc.ac.cn

Chemical composition and source apportionment of PM_{10} and $PM_{2.5}$ in different functional areas of Lanzhou, China

Xionghui Qiu[1,2,3], Lei Duan[1], Jian Gao[2,3,], Shulan Wang[2,3], Fahe Chai[1,2,3,*], Jun Hu[2,3], Jingqiao Zhang[2,3], Yaru Yun[2,3]*

1. *School of Environment, Tsinghua University, Beijing 10084, China*
2. *State Key Laboratory of Environmental Criteria and Risk Assessment, Chinese Research Academy of Environmental Sciences, Beijing 10084, China*
3. *Collaborative Innovation Center of Atmospheric Environment and Equipment Technology, Nanjing 210000, China*

ARTICLE INFO

Article history:
Received 30 May 2015
Revised 14 October 2015
Accepted 15 October 2015
Available online 7 January 2016

Keywords:
Chemical composition
Particulate matter
Source apportionment
Functional areas

ABSTRACT

To elucidate the air pollution characteristics of northern China, airborne PM_{10} (atmospheric dynamic equivalent diameter ≤ 10 μm) and $PM_{2.5}$ (atmospheric dynamic equivalent diameter ≤ 2.5 μm) were sampled in three different functional areas (Yuzhong County, Xigu District and Chengguan District) of Lanzhou, and their chemical composition (elements, ions, carbonaceous species) was analyzed. The results demonstrated that the highest seasonal mean concentrations of PM_{10} (369.48 μg/m^3) and $PM_{2.5}$ (295.42 μg/m^3) were detected in Xigu District in the winter, the lowest concentration of $PM_{2.5}$ (53.15 μg/m^3) was observed in Yuzhong District in the fall and PM_{10} (89.60 μg/m^3) in Xigu District in the fall. The overall average OC/EC (organic carbon/elemental carbon) value was close to the representative OC/EC ratio for coal consumption, implying that the pollution of Lanzhou could be attributed to the burning of coal. The content of SNA (the sum of sulfate, nitrate, ammonium, SNA) in $PM_{2.5}$ in Yuzhong County was generally lower than that at other sites in all seasons. The content of SNA in $PM_{2.5}$ and PM_{10} in Yuzhong County was generally lower than that at other sites in all seasons (0.24–0.38), indicating that the conversion ratios from precursors to secondary aerosols in the low concentration area was slower than in the area with high and intense pollutants. Six primary particulate matter sources were chosen based on positive matrix factorization (PMF) analysis, and emissions from dust, secondary aerosols, and coal burning were identified to be the primary sources responsible for the particle pollution in Lanzhou.

Introduction

Driven by continuous urbanization and industrialization and a rapid growth in energy consumption and the number of motor vehicles, frequent pollution episodes have occurred in most cities. An increasing mass concentration of particulate matter in the atmosphere could have an adverse impact on human health, visibility, and climate change (Xiao et al., 2014b; Ma et al., 2014; Chen et al., 2014; Lawrence and Fatima, 2014). Airborne PM_{10} (atmospheric dynamic equivalent diameter ≤ 10 μm) and $PM_{2.5}$ (atmospheric dynamic equivalent diameter ≤ 2.5 μm) have been reported to be important

* *Corresponding author*. E-mails: gaojian@craes.org.cn (Jian Gao), chaifh@craes.org.cn (Fahe Chai).

http://dx.doi.org/10.1016/j.jes.2015.10.021
1001-0742/

pollutants in China (Huang et al., 2014; Cao et al., 2012). In several reports, the PM_{10} and $PM_{2.5}$ daily concentrations even reached more than 600 and 300 μg/m^3 during the heavy pollution episodes, approximately 4 times the national ambient air quality standard (NAAQS, GB3905-2012) (Sun et al., 2006).

Currently, most of the research on PM focuses on southern China due to its more severe atmospheric environment. The priorities for an air-control area for Chinese administrators were also focused on that region (Sun et al., 2006; Han et al., 2007; Yang et al., 2005b), such as the "National Ten" (Clean Air Action Plan, released by the state council in September, 2013), which regulated that the concentration of $PM_{2.5}$ in the Beijing–Tianjin–Hebei area had to decline by 25%, with 20% for the Yangtze River Delta (YRD), and 15% for the Pearl River Delta (PRD). By contrast, several of the studies and several of the control measures were located in severely polluted cities in northern China or several cities located on rough terrain. Lanzhou is one of the heavily polluted cities in the northwestern region of China. A rapidly deteriorating air environment has been continuously reported because its difficult terrain surrounded by mountains led to unfavorable diffusion conditions (Fan et al., 2014).

The major pollutant in the atmospheric environment of Lanzhou is particulate matter (Xiao et al., 2013, Wang et al., 2007). In recent years, several scholars have begun to investigate the concentration status of particulate matter in Lanzhou (Li et al., 2014; Wang et al., 2014). However, most of these studies focused on concentration changes or a single species variety of $PM_{2.5}$ during the specified period and did not consider the complete chemical composition of the particulate matter, nor did they conduct comparative studies of different functional areas. More importantly, the source of the particulate matter was not noted. As one of the most-developed cities in northwestern China, Lanzhou accommodated more than 433,435 vehicles, a 3.61 million resident population (NBSC, 2013), and heated approximately 100,000,000 m^2/year. Ambiguity in source definition would prevent management departments from taking reasonable and valid measures to control air pollution.

In this study, we considered three typical and representative functional areas: Xigu District (XG, an industrial area), Chengguan District (CG, an urban area), and Yuzhong County (YZ, a rural area) were chosen to identify the chemical characteristics of PM_{10} and $PM_{2.5}$ of the Lanzhou area in three seasons. The concentration variations and chemical composition, as well as possible sources of particulate matter, would be investigated. The results from this study would help the Lanzhou municipal government take scientific and effective measures to alleviate environmental pollution due to particulate matter.

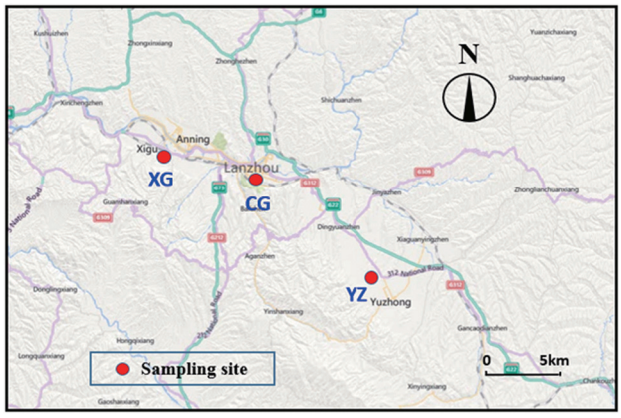

Fig. 1 – Distribution of three representative sampling sites in Lanzhou. XG: Xigu District; CG: Chengguan District; YZ: Yuzhong County.

1. Methods

1.1. Site descriptions

Lanzhou is surrounded by mountains and situated in a valley. The land on which the urban area lies slopes from west to east. The Xigu District (XG, 36°06′00″N, 103°37′48″E) is located to the west of the city. An industrial site, the Xigu District, is surrounded by a number of petrochemical companies and power plants. The Chengguan District (CG, 36°03′00″N, 103°49′48″E) is the political and economic center of Lanzhou with a gathering of population and transportation hubs, where a number of complex pollution sources might be found. The Yuzhong County sampling site (YZ, 35°56′24″N, 104°09′00″E) is 2169 m above the sea level and 600 to 800 m higher than the XG and CG sites. Compared with other sites, anthropogenic sources were rare in the area surrounding YZ. All of the sampling sites were located on the rooftop of three-story buildings (approximately 10 m above the ground). The distribution of sampling sites is indicated in Fig. 1.

1.2. Particulate matter collection

Sample collection was performed simultaneously at all of the sites from May to June and September to October of 2012, and December of 2012 to January of 2013 (Table 1). Each sampling episode was conducted continuously from 8 am to 7 am the next day. A four-channel sampler for PM (TH-150C, Tianhong Instruments Co., Ltd., China) with a flow rate of 28.3 L/min was employed to collect $PM_{2.5}$ and PM_{10}. Both Teflon and Quartz filters were chosen to collect PM for different purposes (the ions and elements were collected on the Teflon filters, the organic and elemental carbon on the Quartz filters). After each sampling episode, the filter membranes were replaced, and the sampler was cleaned with 95% alcohol while the sampling volume was recorded. The filters were transferred to the laboratory and stored at 4°C prior to analysis.

1.3. Sample analysis

1.3.1. Elements

Each Teflon filter sample was divided into 4 equal sections and cut into pieces. The first section was put into a high-pressure Teflon digestion vessel with 6 mL of concentrated HNO_3, 2 mL of concentrated H_2O_2, and 0.1 mL of concentrated HF. Subsequently, a microwave digestion instrument (MD6H, Aopule Instruments Co., Ltd., China) was employed to digest the sample for approximately 45 min. After cooling to room temperature, the sample was heated and evaporated to 0.5 mL on a hot plate. When the sample cooled, the sample was transferred to a 10-mL colorimetric

Table 1 – Sampling information for three functional areas.

Sampling site	Sampling period	Sample	Site description
Xigu	2–25 June 2012	20	Industrial area, many petrochemical plants
	1–23 September 2012	20	
	7 December 2012–1 January 2013	20	
Chengguan	1–22 June 2012	20	Urban, administrative and residential area
	1–23 September 2012	20	
	7 December 2012–2 January 2013	20	
Yuzhong	2–23 June 2012	20	Downwind of Lanzhou, village and farmland
	1–23 September 2012	20	
	7 December 2012–1 January 2013	20	

tube, and 0.2 mL HNO_3 was added for standard calibration. Sixteen elements (Na, Mg, Al, K, Ca, V, Cr, Mn, Fe, Co, Ni, Cu, Zn, As, Cd, and Pb) were determined by inductively coupled plasma-mass spectrometry (ICP-MS) (XSeries^{II}, Thermo, USA). The second section of the filter was put into a nickel crucible and subsequently moved to a muffle furnace, increasing the temperature from room temperature to 300 and 550°C, successively. After adding 0.2 g NaOH to the crucible and reducing the volume to approximately 10 mL at 500°C, then removing the crucible from the muffle furnace and adding 5 mL hot water into it, the solution was extracted and transferred to a plastic tube with 2 mL HCl. The Si and Ti were also determined by inductively coupled plasma-mass spectrometry.

1.3.2. Water-soluble ions

The third section of the filter was immersed into a colorimetric tube with 50 mL purified water and later sonicated for 2 hr. Water-soluble ions were analyzed using an ion chromatograph (IC) (LC-20AD, Shimadzu, Japan) consisting of a separation column and a guard column, a self-regenerating suppressed conductivity detector and a gradient pump.

1.3.3. Organic carbon/elemental carbon

The organic carbon (OC) and elemental carbon (EC) from the Quartz filters were determined by a Thermal/Optical carbon analyzer (DRI2001A, Desert Research Institute, USA). A 1.5 cm^2 punch of a sample quartz filter was heated stepwise in a nonoxidizing helium atmosphere to volatilize the organics and then heated in an oxidizing atmosphere of 2% oxygen in a balance of helium to burn out the elemental carbon. The organics were converted into CH_4 by an oxidation and reduction reaction, and a flame ionization detector (FID) was subsequently employed to quantify the monitored values. A 633 nm He–Ne laser was used to confirm the split-off point of OC/EC by monitoring the change in the light intensity during the heating process.

1.4. PMF model analysis

Positive matrix factorization (PMF) v3.0, an advanced factor analysis technique based on a weighted least squares fit approach (Paatero, 1997), was employed to identify and quantify the major aerosol sources. The PMF approach used realistic error estimates to weigh data values and impose non-negativity constraints in the factor computational process. The PMF factor model can be written as

$$X = G \times F + E$$

where, X is a known n by m matrix of the m measured chemical species in n samples, G is the $n \times p$ source score matrix of the nth sample pth factor, F is the $p \times m$ source loading matrix of the mth species in the pth factor, and E is the residual. The PMF model has been widely used to identify possible sources for various aerosol constituents (Shen et al., 2011; Nguyen et al., 2013).

2. Results and discussion

2.1. Spatial variations of $PM_{2.5}$ and PM_{10} mass concentration

The seasonal average $PM_{2.5}$ and PM_{10} concentrations for three sampling sites are presented in Fig. 2. The highest seasonal mean concentrations of PM_{10} and $PM_{2.5}$ were detected in XG in the winter (295.42 $\mu g/m^3$ for $PM_{2.5}$ and 369.89 $\mu g/m^3$ for PM_{10}, respectively). The lowest concentration of $PM_{2.5}$ was observed in YZ in the fall (53.15 $\mu g/m^3$), and the lowest concentration of PM_{10} was observed in XG in the fall. These results could be explained by the extensive burning of coal for domestic heating. In addition, in the winter, the atmosphere was controlled by the presence of high-pressure systems and highly stable atmospheric conditions, often associated with subsidence inversion, resulting in the accumulation of atmospheric pollutants (Xu et al., 2009; Cao et al., 2005; Xiao et al., 2014a). For YZ, the $PM_{2.5}$ and PM_{10} levels (110.27 $\mu g/m^3$ for $PM_{2.5}$ and 174.25 $\mu g/m^3$ for PM_{10}, respectively) were found to be considerably higher than in XG (88.88 $\mu g/m^3$ for $PM_{2.5}$ and 150.15 $\mu g/m^3$ for PM_{10}, respectively) and CG (53.16 $\mu g/m^3$ for $PM_{2.5}$ and 109.25 $\mu g/m^3$ for PM_{10}), even if only sporadic and insignificant pollution sources existed in these areas. According to the weather data from the Lanzhou meteorological administrator (LMA, 2012) and other literature (Xiao et al., 2012; Fan et al., 2014), higher wind speed was found in the summer (most days above 2.5 m/sec), indicating that the reason for the observed values might relate to the prevailing wind speed. YZ was significantly influenced by the flow of pollution from its surrounding cities under the prevailing northwest winds. On the other hand, Lanzhou is located on the Loess Plateau and because of the sharp wind in summer, dust aerosols were easily produced. These dust aerosols were the result of the combination of the two factors mentioned above. In the fall, the concentration of PM_{10} in the three functional areas was observed to be similar (differences within 10%, 96.79 $\mu g/m^3$ in YZ, 89.60 $\mu g/m^3$ in XG, and 93.40 $\mu g/m^3$ in CG), but the concentration of $PM_{2.5}$ in XG (79.72 $\mu g/m^3$) was observed to be significantly higher than in YZ (53.15 $\mu g/m^3$) and CG (54.95 $\mu g/m^3$). XG is an industrial area as defined by local administration, with continuous, massive and varied pollutants intensively discharged over an extended time period. These pollutants were difficult to diffuse or dilute due to the adverse weather conditions. Furthermore, the wet atmospheric environment in the fall was conducive to the formation of secondary

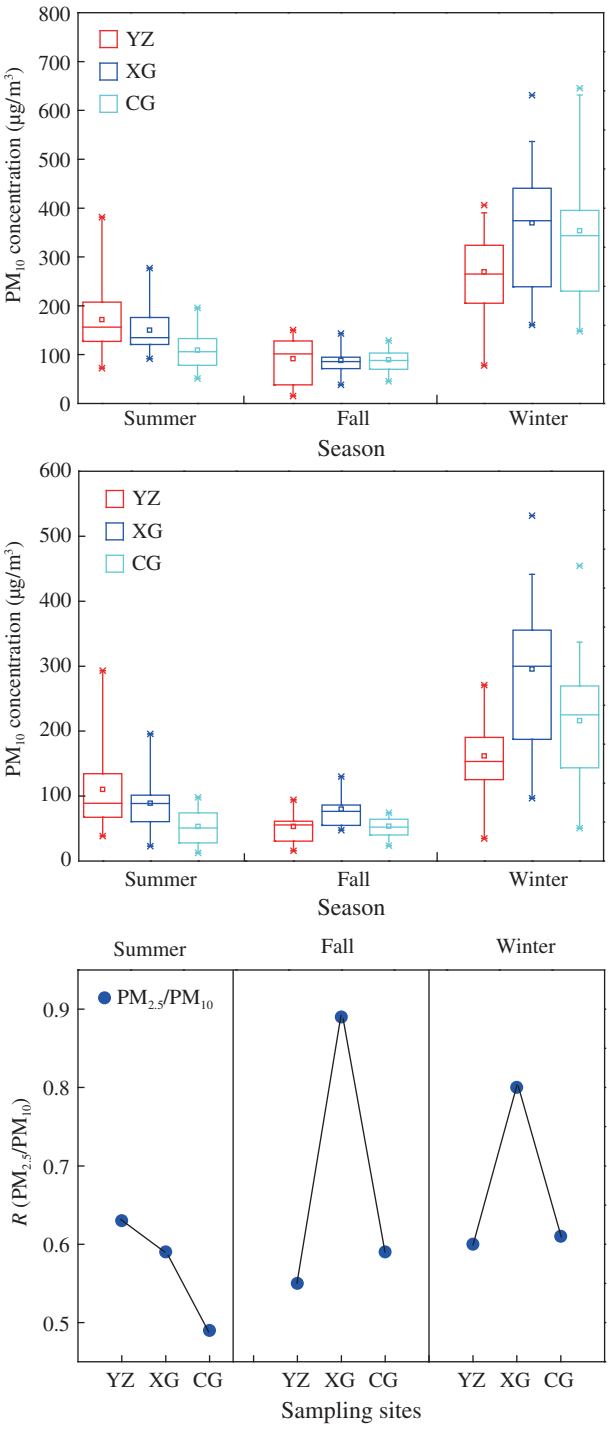

Fig. 2 – Concentration distribution of PM_{10} and $PM_{2.5}$ in three functional areas and the ratios of $PM_{2.5}/PM_{10}$ (*R*) in three functional areas.

aerosols. In addition, the daily concentration peak of $PM_{2.5}$ was 531.64 μg/m^3 in XG, which exceeded the new national ambient air quality standard (NAQQS, 75 μg/m^3) by more than a factor of 7. The highest concentration of PM_{10} was 645.27 μg/m^3 in CG, where the level was four-fold higher than the NAQQS (150 μg/m^3). Indicating heavy air pollution in Lanzhou, these monitored values were even far above the Chinese main air control area, YRD and PRD, in the same period (Wang et al., 2013), which also should attract the attention of the National Ministry of Environmental Protection and the local government.

The ratio (*R*) of $PM_{2.5}/PM_{10}$ could reflect the main atmospheric particulate matter pollution. In this study, *R* ranged from 0.60 to 0.80 in the winter, indicating that $PM_{2.5}$ was the primary pollutant in the winter, which also further explained the easier formation of secondary aerosols during the heavy pollution period. Except for XG, *R* in the summer and the fall was somewhat lower than in the winter. Additionally, as previously mentioned, the high concentration of pollutants discharged from industries in XG accumulated and converted into secondary aerosols under favorable weather conditions.

2.2. Seasonal variations of $PM_{2.5}$ and PM_{10} chemical species in three functional areas

2.2.1. Carbonaceous species

Fig. 3 shows the seasonal variation of the carbonaceous species in the three functional areas. The highest OC seasonal average concentration for $PM_{2.5}$ was 47.21 μg/m^3 in CG in winter. The maximum OC concentration in PM_{10} (58.98 μg/m^3) was also detected in this functional area. The minimum OC concentrations in $PM_{2.5}$ and PM_{10} were both found in YZ in the fall (4.23 μg/m^3 for $PM_{2.5}$, 4.75 μg/m^3 for PM_{10}). There was approximately a factor of 10 difference between the peak and valley values for OC in either $PM_{2.5}$ or PM_{10}. The highest seasonal average concentrations of EC and OC in $PM_{2.5}$ and PM_{10} for all functional areas were observed in the winter (4.3–9.4 μg/m^3 for $PM_{2.5}$, 6.06–12.1 μg/m^3 for PM_{10}), surpassing their concentrations in the fall by approximately a factor of 4–8. This study suggested that the difference was the result of coal burning. The same phenomenon of high OC and EC levels was detected in northern cities such as Urumqi and Xi'an (Yang et al., 2011; Shen et al., 2014). The OC and EC levels in CG were always higher than in YZ and XG, which could relate to the large numbers of people living in the area and their activities. Moreover, transportation was an important OC emission source in the center of the cities. A monitoring result at an urban traffic site identified that OM plus EC in $PM_{2.5}$ reached up to 54.8% in Greece (Samara et al., 2014).

The ratio of OC/EC for $PM_{2.5}$ has been employed as an indicator of sources. The defined values were 1.1, 2.7 and 9.0, representing vehicle emissions, coal combustion and biomass burning, respectively (Cachier and Ducret, 1991; Watson et al., 2001). In this study, the seasonal average of OC/EC decreased in the order of winter (4.78) > summer (2.91) > fall (2.70). The overall average OC/EC was 3.46, a value close to the representative OC/EC ratio of coal consumption, implying that the pollution of Lanzhou was attributable to coal burning. These results were also similar to the results observed in a study in heavily polluted urban Urumqi (the capital of Xinjiang Province, near Gansu province) (Li et al., 2008). The OC/EC value for PM_{10} was close to or a little lower than the ratio for $PM_{2.5}$, suggesting the same correlation with a different particle diameter.

The average TC (total carbon)/$PM_{2.5}$ decreased in the order of winter (0.19) > summer (0.15) > fall (0.13) for $PM_{2.5}$ and winter (0.16) > fall (0.11) = summer (0.11) for TC/PM_{10}. The ratio of TC/PM ($PM_{2.5}$ or PM_{10}) in CG was observed with greater persistence than in YZ and XG because of the impact of motor vehicle emissions on the chemical composition of

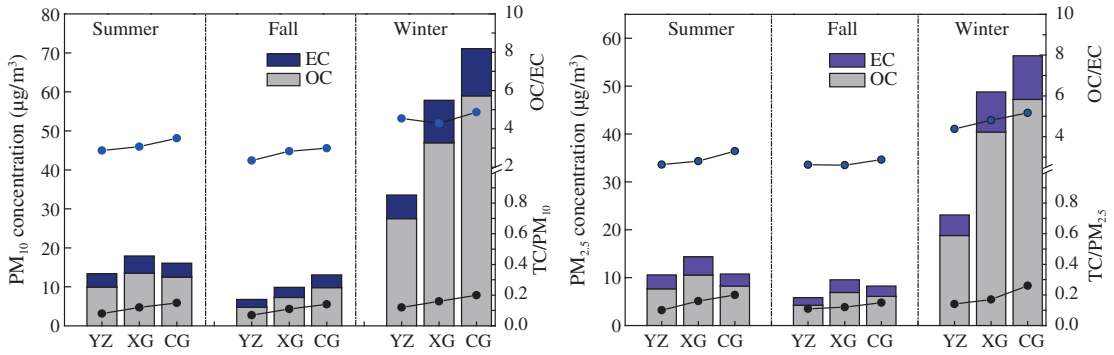

Fig. 3 – Seasonal average concentrations of carbonaceous species in PM_{10}, TC/PM_{10}, OC/EC, $PM_{2.5}$, $TC/PM_{2.5}$, and OC/EC in three functional areas. TC: total carbon; OC: organic carbon; EC: element carbon.

the particulate matter. A somewhat lower TC/PM ($PM_{2.5}$ or PM_{10}) ratio (0.10–0.14 for $PM_{2.5}$, 0.07–0.12 for PM_{10}) was always found in YZ in the same period, identified as the carbonaceous particles produced primarily by human activities.

2.2.2. Sulfate, nitrate and ammonium

This study focused primarily on the inorganic ions SNA (the sum of sulfate, nitrate and ammonium). The seasonal average concentration of SNA in $PM_{2.5}$ and PM_{10} at three sites is shown in Fig. 4. Generally, the content of SNA in $PM_{2.5}$ and PM_{10} was significantly higher in the winter than in the other seasons, indicating easier formation of secondary aerosols under the weather conditions of winter. The average values of SNA in all three sites were calculated as winter (0.35) > fall (0.26) > summer (0.24). In addition, the content of ∑SNA in $PM_{2.5}$ in YZ (0.2–0.32) was generally lower than at other sites in all seasons (0.24–0.38). This difference might be explained as the conversion ratios in a low concentration area from precursors to secondary aerosols being slower than the conversion ratios in an area with high and intensive pollutants. SNA was closely related to economic progress in China. Numerous reports confirmed that SNA was characteristic of regional fine particulate pollution in Beijing–Tianjin–Hebei, YRD and PRD because of their developed economy (Xu et al., 2002; Wang et al., 2013; Yang et al., 2005a). In a coastal site of northern Spain, results are summarized as 28.0% SNA in PM_{10} and 33.4% in $PM_{2.5}$ (Salvador et al., 2007), which could lead to the conclusion that the pollution sources in Spain were typically associated with anthropogenic emissions. Consistent results were obtained in other research in European countries (Putaud et al., 2007) such as in Monagrega (Spain), Illmitz (Austria) and Chaumont (Switzerland).

The ratio of NO_3^-/SO_4^{2-} has been employed as an indicator of the importance of stationary and mobile sources for production of sulfate and nitrogen (Wang et al., 2015; Yao et al., 2002). The average NO_3^-/SO_4^{2-} ratio for $PM_{2.5}$ in three seasons was fall (0.48) > winter (0.34) > summer (0.31), indicating that a greater proportion of $PM_{2.5}$ was from motor vehicle exhaust in the fall compared with other seasons. The ratio of NO_3^-/SO_4^{2-} from $PM_{2.5}$ and PM_{10} in YZ in the winter (0.44 for $PM_{2.5}$, 0.43 for PM_{10}) was found to be greater than in XG (0.26 for $PM_{2.5}$, 0.27 for PM_{10}) and YZ (0.33 for $PM_{2.5}$, 0.33 for PM_{10}). Because more SO_2 than NO_x was discharged in XG and CG, the motor vehicle emissions for NO_x in CG were greater than the motor vehicle emissions in XG.

The degree of sulfate neutralization (DON) was employed to estimate whether sulfate was completely acidic, fully neutralized by ammonia, or in between. All the terms in the DON equation was expressed in unit of $\mu g/m^3$ (Chen et al., 2014):

$$DON = \left(\frac{[NH_4^+]}{18} - \frac{[NO_3^-]}{62}\right) \times \left(\frac{[SO_4^{2-}]}{96}\right)^{-1}.$$

If sulfate were fully neutralized in the form of ammonium sulfate, that would mean 2 mol ammonia for every mole of sulfate, and the DON value could be defined as 2. Similarly, DON was 1 when sulfate was ammonium bisulfate, and DON was 0 when sulfate was particulate sulfuric acid. The equation above is based on the assumption that nitrate was only neutralized by ammonia, although the results might be affected by other ions (such as Cl^- and Ca^{2+}). At some level, this factor could explain the formation of secondary aerosols at the three sampling sites.

Table 2 demonstrates the DON values in the three functional areas. Most of the DON values ranged from 1 to 2, indicating the formation of ammonium sulfate or ammonium bisulfate. In the winter, the detected DON values of Lanzhou were mostly close to 2, which was explained as ammonium sulfate possibly being easier to produce. By calculating DON values from other research, Urumqi was 1.6 in the winter of 2007, and Lanzhou was 1.5 in the winter of 2007 (Li et al., 2008; She, 2011). All of this evidence demonstrated formation of ammonium sulfate in the winter. In addition, the DON value in YZ was significantly lower than in XG and CG in the fall and winter (the difference between YZ and XG in summer was small), indicating that it was more favorable to form ammonium sulfate or ammonium bisulfate with rather high SO_2 emissions. The DON value in YZ in the fall was 0.85. This result supported easier production of ammonium bisulfate or particulate sulfuric acid.

2.2.3. Element

The eighteen tested elements (Na, Mg, Al, Si, K, Ca, Ti, V, Cr, Mn, Fe, Co, Ni, Cu, Zn, As, Cd, and Pb) in $PM_{2.5}$ and PM_{10} were detected at the three functional areas. In total, these elements

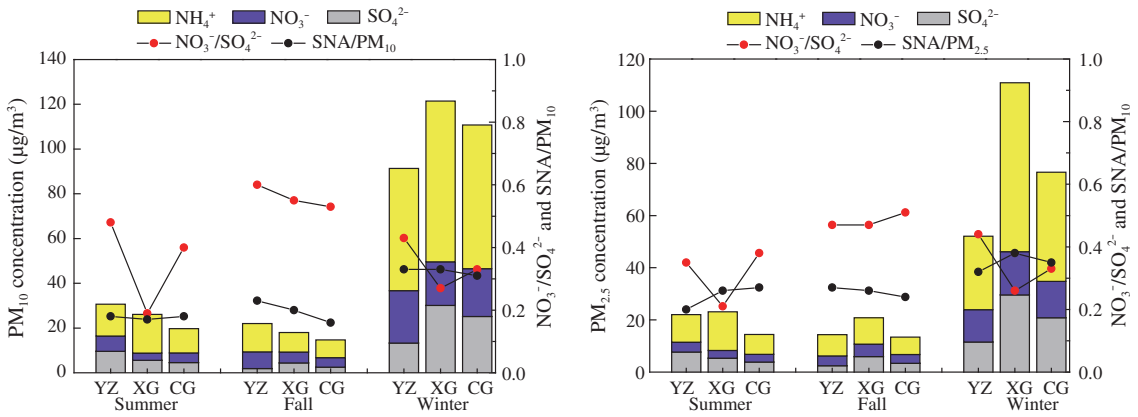

Fig. 4 – Seasonal average inorganic ions in PM_{10} and $PM_{2.5}$ in three functional areas. SNA: the sum of sulfate, nitrate, ammonium.

in $PM_{2.5}$ (14%–22%) or PM_{10} (16%–31%) showed no obvious differences in different seasons and functional areas. Mg, Al, Si, Ca, Mn and Fe have been most often considered as the indicators of mineral dust sources. From Fig. 5, the six elements accounted for 80%–90% in $PM_{2.5}$ and PM_{10}, indicating that dust was most probably the main source. At the Tongliao site, located in the center of Horqin in Inner Mongolia, the fraction of mineral dust in $PM_{2.5}$ reached up to 43% during the period of dust storms in spring in 2005 (Shen et al., 2007). The crustal material in Beijing constituted 18.6% of $PM_{2.5}$ mass but soared to 41.6% when sand dust invaded (Yang et al., 2005b), revealing that sandstorm breakout was distinctive in northern China.

In addition, Pb was generally enriched in the aerosol as a result of emissions from gasoline additives (Xu et al., 2012). The concentration of Pb in CG was significantly higher than in YZ and XG. In the summer and the fall, the percentages of Pb in $PM_{2.5}$ in CG were 0.18% and 0.40%, respectively, 5–6 times the values in YZ. By contrast, the ratio was calculated as 0.16% in the winter, just 2.6 times the value in YZ. These values would be affected by the burning of coal for heating in the winter (Pb was also enriched in the coal). Similar results were detected for PM_{10}. Zn was considered as the indicator of an industrial source (Dall'Osto et al., 2013). From the monitoring results, the percentage of Zn in $PM_{2.5}$ and PM_{10} in XG was significantly higher than in YZ and slightly greater than in CG, implying that some industrial sources might be distributed in CG. Moreover, the content of Zn in $PM_{2.5}$ and PM_{10} in the fall and the winter was significantly above the values observed in the summer, which also indicated more human activities and industrial processes. As was used to define enriched emissions from coal burning (Tian et al., 2011). The content ranged from 4.95×10^{-4}–6.28×10^{-4} for $PM_{2.5}$ and 1.46×10^{-3}–1.72×10^{-3} for PM_{10} in the summer, sharply increasing to 2.38×10^{-3}–6.03×10^{-3} for $PM_{2.5}$ and 4.59×10^{-3}–6.78×10^{-3} for PM_{10} in the winter.

2.3. $PM_{2.5}$ and PM_{10} source apportionment

The chemical composition of six factors was chosen to determine the source of $PM_{2.5}$ and PM_{10} using the PMF (EPA PMF3.0 version). Fig. 6 presents the source apportionment results for the three functional areas and all samples based on data from three seasons. Eight potential sources chosen by the model included coal burning, secondary aerosols, dust related, traffic, industry and others.

Eight factors were decided by representative indicators. The coal burning source was highly loaded with SO_4^{2-}, OC, EC, and As (Tian et al., 2011). In northwestern China, the coal burning source was generally associated with extensive burning for domestic heating. The secondary aerosol source was loaded with SO_4^{2-} and NO_3^-, which originated from chemical conversion from primary SO_2 and NO_x generated by other direct sources. The dust-related source was loaded with Ca, Mg, Si, Al, Fe (Shen et al., 2011), which were generated from crustal material and

Table 2 – Value of sulfate, nitrate and ammonium and the degree of sulfate neutralization (DON) value for $PM_{2.5}$.

Season	Sampling site	$PM_{2.5}$ (μg/m³)	NH_4^+ (mol)	NO_3^- (mol)	SO_4^{2-} (mol)	DON
Summer	Yuzhong	110.27	4.69	3.75	10.59	1.66
	Xigu	87.63	5.29	3.03	14.79	1.59
	Chengguan	53.16	3.84	2.94	7.65	2.08
Fall	Yuzhong	53.15	2.41	3.81	8.16	0.86
	Xigu	79.72	5.94	4.75	10.15	2.40
	Chengguan	54.95	3.34	3.41	6.67	1.88
Winter	Yuzhong	164.84	11.51	12.44	28.16	1.50
	Xigu	295.42	29.61	16.54	64.73	2.04
	Chengguan	216.73	20.85	13.93	41.85	2.14

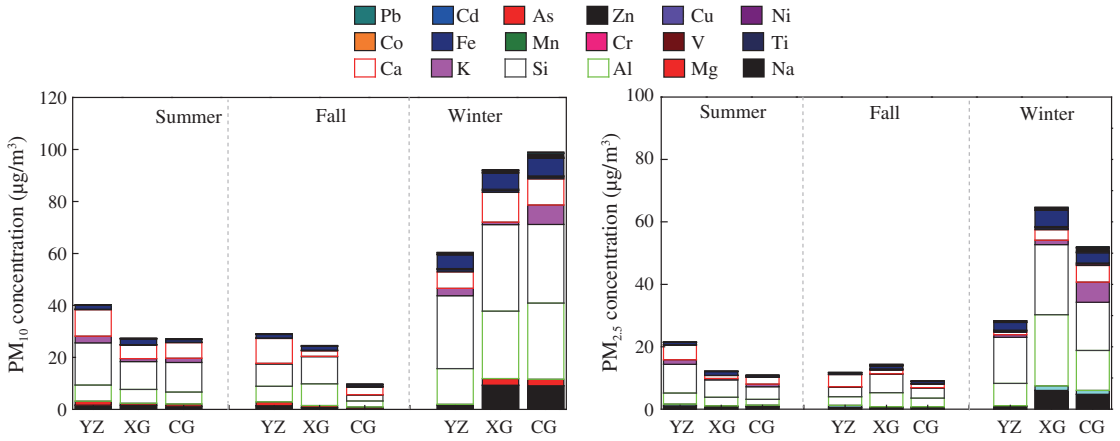

Fig. 5 – Seasonal average inorganic elements in PM_{10} and $PM_{2.5}$ in three functional areas.

fugitive dust. The traffic source was typically characterized by NO_3^-, EC and Pb (Dall'Osto et al., 2013). The industrial source was typically characterized by high concentrations of the trace elements Zn and Cr. These elements were enriched in aerosols as a result of emissions from smelters and metallurgical industries (Dall'Osto et al., 2013). The others included some undefined or unknown emission sources.

The source apportionment results for six factors in the three representative functional areas with no intense emission source areas, an industrial area and a complex emission area are shown in Fig. 6. For the non-intensive emission source area YZ site, the sources for PM_{10} and $PM_{2.5}$ in decreasing order were dust related (38.9%) > secondary aerosols (22.7%) > others (15.9%) > coal burning (13.3%) > traffic (4.9%) > industry (4.3%) and dust related (37.7%) > secondary aerosols (25.5%) > coal burning (17.0%) > others (9.2%) > traffic (5.6%) > industry (5.0%), respectively. For the industrial area XG site, the decreasing order of sources for PM_{10} and $PM_{2.5}$ was dust related (29.8%) > secondary aerosols (23.6%) > coal burning (18.7%) > traffic (15.3%) > industry (8.4%) > others (4.2%) and dust related (26.3%) > secondary aerosols (25.2%) > coal burning (20.1%) > traffic (16.1%) > industry (9.2%) > others (3.1%), respectively. In the complex source CG site, the order of the sources from largest to smallest was secondary aerosols (27.3%) > coal burning (21.0%) > dust related (20.4%) > traffic (20.1%) > industry (7.8%) > others (3.4%) and secondary aerosols (28.8%) > coal burning (21.2%) > traffic (21.2%) > dust related (17.6%) > industry (9.0%) > others (3.9%), respectively. From the above source apportionment results, the dust-related contribution was apparently higher than other contributions in the three functional areas, which would be related to the special geographic position and meteorological conditions (Xiao et al., 2014b). First, the dust related source would be transported from the adjacent desert region. The back trajectory model had been employed to

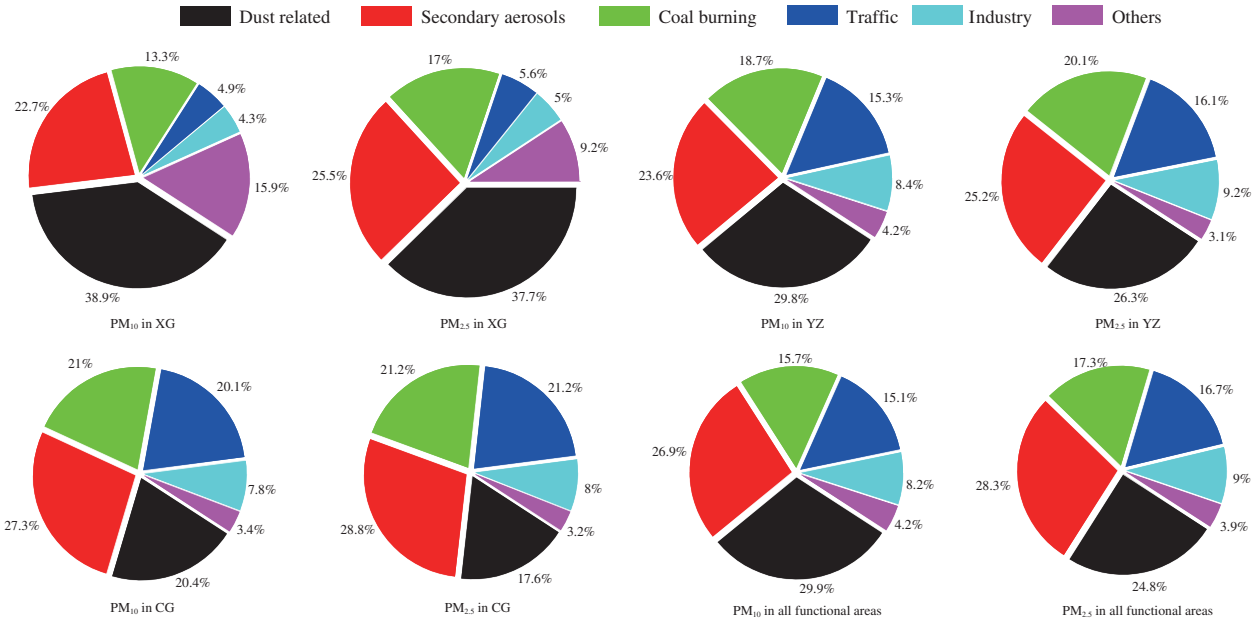

Fig. 6 – Source apportionment of PM_{10} and $PM_{2.5}$ in YZ, XG, CG and all functional areas.

conclude that particle transport could easily affect the air quality in northwestern China (Cao et al., 2012). Additionally, Lanzhou is located on the Loess Plateau, with a lower green coverage rate, which would lead to increasing dust concentrations when the wind speed was high.

In total, the percentage of secondary aerosols in all three functional areas accounted for more than 20%, indicating that the weather conditions were favorable for chemical conversion of primary pollutants. From other research, because of the special terrain around Lanzhou, the mountains prevented the rapid diffusion of pollutants in the atmospheric environment. Long-term retention of these primary pollutants resulted in easier formation of secondary aerosols (Fan et al., 2014). The source apportionment results showed the typical characteristics of the three functional areas. The highest content from a dust-related source was found in YZ, indicating that the main source was generated by crustal material in the non-intensive emission source area. The highest industrial contribution was detected in XG, but its content was just slightly higher than other functional areas, indicating that the industrial source was not dominant, the traffic source in CG was calculated to be significantly greater than in YZ and XG. The contribution of the dust source was obviously lower than in these areas, indicating that a more complex and intensive emission source might be included with more serious vehicle pollution in this area.

From the source apportionment results for all samples for PM_{10} and $PM_{2.5}$, the proportion in decreasing order was dust-related (29.8%) > secondary aerosols (26.9%) > coal burning (15.7%) > traffic (15.1%) > industry (8.2%) > others (4.2%) and secondary aerosols (28.3%) > dust related (26.9%) > coal burning (17.3%) > traffic (16.7%) > industry (9.0%) > others (3.9%). These results from PMF analysis were close to the results from an earlier study (Jin, 2014). Moreover, PMF analysis indicated that the dust-related source, secondary aerosol source and coal burning were the major sources, with results consistent with those from several studies in other cities of northwestern China (Cao et al., 2012; Wu et al., 2015; Shi et al., 2015), revealing that the pollution from dust, secondary aerosols and coal burning were common features in the cities of northwestern China.

3. Conclusions

The highest seasonal mean concentrations of PM_{10} and $PM_{2.5}$ were detected in XG in the winter (295.42 $\mu g/m^3$ for $PM_{2.5}$ and 369.89 $\mu g/m^3$ for PM_{10}, respectively). The lowest concentration of $PM_{2.5}$ was observed in YZ in the fall (53.15 $\mu g/m^3$) and for PM_{10} in XG in the fall. The overall average OC/EC value was close to the representative OC/EC ratio for coal consumption, implying that the pollution of Lanzhou was attributable to the burning of coal. The content of SNA in $PM_{2.5}$ in YZ was generally lower than other sites in all seasons. The highest average NO_3^-/SO_4^{2-} ratio for $PM_{2.5}$ in the three seasons was in fall. The DON value revealed easier formation of ammonium sulfate in the winter.

Six sources for PM_{10} and $PM_{2.5}$ were calculated by the PMF analysis, *i.e.*, coal burning, secondary aerosols, dust related, traffic, industry and others. The source apportionment supported the conclusion that emissions from dust related, secondary aerosols, and coal burning were the main reasons for particulate matter pollution in Lanzhou.

Acknowledgments

This study was supported by the Special Scientific Research Funds for Environment Protection Commonweal Section (Nos. 201409003, 201309011), the National Natural Science Foundation of China (No. 41375132), the CAS Strategic Priority Research Program (No. XDB05030400), the National Basic Research Program of China (No. 2014CB441203) and the Beijing Municipal Science and Technology Plan (No. Z131100006113013). We thank the staff of the local environmental authority in the three sites for their assistance in sampling, and also thank the anonymous reviewers for their helpful comments and corrections in the manuscript.

REFERENCES

Cachier, H., Ducret, J., 1991. Influence of biomass burning on equatorial African rains. Nature 352 (6332), 228–230.

Cao, J.J., Wu, F., Chow, J.C., Lee, S.C., Li, Y., Chen, S.W., et al., 2005. Characterization and source apportionment of atmospheric organic and elemental carbon during fall and winter of 2003 in Xi'an. China. Atmos. Chem. Phys. 5 (11), 3127–3137.

Cao, J.J., Wang, Q.Y., Chow, J.C., Watson, J.G., Tie, X.X., Shen, Z.X., et al., 2012. Impacts of aerosol compositions on visibility impairment in Xi'an. China. Atmos. Environ. 59, 559–566.

Chen, T.F., Chang, K.H., Tsai, C.Y., 2014. Modeling direct and indirect effect of long range transport on atmospheric $PM_{2.5}$ levels. Atmos. Environ. 89, 1–9.

Dall'Osto, M., Querol, X., Alastuey, A., O'Dowd, C., Harrison, R.M., Wenger, J., et al., 2013. On the spatial distribution and evolution of ultrafine particles in Barcelona. Atmos. Chem. Phys. 13 (2), 741–759.

Fan, J., Yue, X.Y., Yi, J., Chen, Q., Wang, S.G., 2014. Online monitoring of water-soluble ionic composition of PM_{10} during early summer over Lanzhou City. J. Environ. Sci. 26 (2), 353–361.

Han, L.H., Zhuang, G.S., Cheng, S.Y., Wang, Y., Li, J., 2007. Characteristics of re-suspended road dust and its impact on the atmospheric environment in Beijing. Atmos. Environ. 41 (35), 7485–7499.

Huang, R.J., Zhang, Y.L., Bozzetti, C., Ho, K.F., Cao, J.J., Han, Y., et al., 2014. High secondary aerosol contribution to particulate pollution during haze events in China. Nature 514 (7521), 218–222.

Jin, Y., 2014. The source profiles replacement and receptor data expansion and their application in source apportionment of PM10 in Lanzhou MSc thesis Lanzhou University, Lanzhou, China.

Lanzhou Meteorological Administration (LMA), 2012. The weather report data in Lanzhou. http://qxj.lanzhou.gov.cn/.

Lawrence, A., Fatima, N., 2014. Urban air pollution & its assessment in Lucknow City—the second largest city of North India. Sci. Total Environ. 488–489, 447–455.

Li, J., Zhuang, G.S., Huang, K., Lin, Y.F., Xu, C., Yu, S.L., 2008. Characteristics and sources of air-borne particulate in Urumqi, China, the upstream area of Asia dust. Atmos. Environ. 42 (4), 776–787.

Li, G., Shi, G.Y., Li, H.Y., Deng, Z.Q., 2014. Pollution characteristics of carbonaceous aerosols in PM2.5 during winter in Lanzhou. J. Univ. Chin. Acad. Sci. 31 (3), 439–443.

Ma, J., Chen, L.L., Guo, Y., Wu, Q., Yang, M., Wu, M.H., et al., 2014. Phthalate diesters in Airborne $PM_{2.5}$ and PM_{10} in a suburban

area of Shanghai: seasonal distribution and risk assessment. Sci. Total Environ. 497–498, 467–474.
NBSC, 2013. China Statistical Yearbook. Chinese Statistics Press, Beijing.
Nguyen, Q.T., Skov, H., Sørensen, L.L., Jensen, B.J., Grube, A.G., Massling, A., et al., 2013. Source apportionment of particles at Station Nord, North East Greenland during 2008–2010 using COPREM and PMF analysis. Atmos. Chem. Phys. 13 (1), 35–49.
Paatero, P., 1997. Least squares formulation of robust non-negative factor analysis. Chemom. Intell. Lab. Syst. 37 (1), 23–35.
Putaud, J.P., Raes, F., Van-Dingenen, R., Brüggemann, E., Facchini, M.C., Decesari, S., et al., 2007. A European aerosol phenomenology-2: chemical characteristics of particulate matter at kerbside, urban, rural and background sites in Europe. Atmos. Environ. 38 (16), 2579–2595.
Salvador, P., Artiñano, B., Querol, X., Alastuey, A., Costoya, M., 2007. Characterisation of local and external contributions of atmospheric particulate matter at a background coastal site. Atmos. Environ. 41 (1), 1–17.
Samara, C., Voutsa, D., Kouras, A., Eleftheriadis, K., Maggos, T., Saraga, D., et al., 2014. Organic and elemental carbon associated to PM_{10} and $PM_{2.5}$ at urban sites of northern Greece. Environ. Sci. Pollut. Res. 21 (3), 1769–1785.
She, F., 2011. A study on chemical characteristics of particulate matters in Lanzhou area and influence of dust event on them PhD thesis Lanzhou University, Lanzhou, China.
Shen, Z.X., Cao, J.J., Arimoto, R., Zhang, J., Jie, D.M., Liu, S.X., et al., 2007. Chemical composition and source characterization of spring aerosol over Horqin sand land in northeastern China. J. Geophys. Res. 112 (14), D14315.
Shen, Z.X., Cao, J.J., Liu, S.X., Zhu, C.S., Wang, X., Zhang, T., et al., 2011. Chemical composition of PM_{10} and $PM_{2.5}$ collected at ground level and 100 meters during a strong winter-time pollution episode in Xi'an, China. J. Air Waste Manage. Assoc. 61 (11), 1150–1159.
Shen, Z.X., Cao, J.J., Zhang, L.M., Liu, L., Zhang, Q., Li, J.J., et al., 2014. Day–night differences and seasonal variations of chemical species in PM_{10} over Xi'an, northwest China. Environ. Sci. Pollut. Res. 21 (5), 3697–3705.
Shi, J.W., Deng, H., Bai, Z.P., Kong, S.F., Wang, X.Y., Hao, J.M., et al., 2015. Emission and profile characteristic of volatile organic compounds emitted from coke production, iron smelt, heating station and power plant in Liaoning Province. China. Sci. Total Environ. 515–516, 101–108.
Sun, Y., Zhuang, G.S., Zhang, W.J., Wang, Y., Zhuang, Y.H., 2006. Characteristics and sources of lead pollution after phasing out leaded gasoline in Beijing. Atmos. Environ. 40 (16), 2973–2985.
Tian, H.Z., Wang, Y., Xue, Z.G., Qu, Y.P., Chai, F.H., Hao, J.M., 2011. Atmospheric emissions estimation of Hg, As, and Se from coal-fired power plants in China, 2007. Sci. Total Environ. 409 (16), 3078–3081.
Wang, S.G., Yuan, W., Shang, K.Z., 2007. The impacts of different kinds of dust events on PM_{10} pollution in northern China. Atmos. Environ. 40 (40), 7975–7982.
Wang, J., Hu, Z.M., Chen, Y.Y., Chen, Z.L., Xu, S.Y., 2013. Contamination characteristics and possible sources of PM_{10} and $PM_{2.5}$ indifferent functional areas of Shanghai. China. Atmos. Environ. 68, 221–229.
Wang, F., Chen, Q., Zhang, W.Y., Guo, Y.T., Zhao, L.B., 2014. Effect of sand dust weather on major water-soluble ions in PM_{10} in Lanzhou. China Environ. Sci. 35 (7), 2477–2482.
Wang, P., Cao, J.J., Shen, Z.X., Han, Y.M., Lee, S.C., Huang, Y., et al., 2015. Spatial and seasonal variations of $PM_{2.5}$ mass and species during 2010 in Xi'an, China. Sci. Total Environ. 508, 477–487.
Watson, J.G., Chow, J.C., Houck, J.E., 2001. $PM_{2.5}$ chemical source profiles for vehicle exhaust, vegetative burning, geological material, and coal burning in Northwestern Colorado during 1995. Chemosphere 43 (8), 1141–1151.
Wu, H., Zhang, Y.F., Han, S.Q., Wu, J.H., Bi, X.H., Shi, G.L., et al., 2015. Vertical characteristics of $PM_{2.5}$ during the heating season in Tianjin, China. Sci 523, 152–160.
Xiao, Z.H., Shao, L.Y., Zhang, N., 2012. Physical and chemical characteristics of airborne particles and its effect on health in Lanzhou. China University of Mining and Technology Press.
Xiao, Z.H., Shao, L.Y., Zhang, N., Wang, J., Wang, J.Y., 2013. Heavy metal compositions and bioreactivity of airborne PM_{10} in a valley-shaped city in northwestern China. Aerosol Air Qual. Res. 13 (3), 1116–1125.
Xiao, S., Wang, Q.Y., Cao, J.J., Huang, R.J., Chen, W.D., Han, Y.M., et al., 2014a. Long-term trends in visibility and impacts of aerosol composition on visibility impairment in Baoji. China. Atmos. Res. 149, 88–95.
Xiao, Z.H., Shao, L.Y., Zhang, N., Wang, J., Chuang, H.C., Deng, Z.Z., et al., 2014b. A toxicological study of inhalable particulates in an industrial region of Lanzhou City, northwestern China: results from plasmid scission assay. Aeolian Res. 14, 25–34.
Xu, J., Bergin, M.H., Yu, X., Liu, G., Zhao, J., Carrico, C.M., et al., 2002. Measurement of aerosol chemical, physical and radiative properties in the Yangtze delta region of China. Atmos. Environ. 36 (2), 161–173.
Xu, H., Wang, Y., Wen, T., Yang, Y., Zhao, Y., 2009. Characteristics and source apportionment of atmospheric aerosols at the summit of Mount Tai during summertime. Atmos. Chem. Phys. Discuss. 9 (4), 16361–16379.
Xu, H.M., Cao, J.J., Ho, K.F., Ding, H., Han, Y.M., Wang, G.H., et al., 2012. Lead concentrations in fine particulate matter after the phasing out of leaded gasoline in Xi'an. China. Atmos. Environ. 46, 217–224.
Yang, H., Yu, J.Z., Ho, S.S.H., Xu, J.H., Wu, W.S., Wan, C.H., et al., 2005a. The chemical composition of inorganic and carbonaceous materials in $PM_{2.5}$ in Nanjing, China. Atmos. Environ. 39 (20), 3735–3749.
Yang, F.M., Ye, B.M., He, K.B., Ma, Y.L., Cadle, S.H., Chan, T., et al., 2005b. Characterization of atmospheric mineral components of $PM_{2.5}$ in Beijing and Shanghai, China. Sci. Sci. Total Environ. 343 (1–3), 221–230.
Yang, F., Tan, J., Zhao, Q., Du, Z., He, K., et al., 2011. Characteristics of $PM_{2.5}$ speciation in representative megacities and across China. Atmos. Chem. Phys. 11 (11), 5207–5219.
Yao, X.H., Chan, C.K., Fang, M., Cadle, S., Chan, T., Mulawa, P., et al., 2002. The water-soluble ionic composition of $PM_{2.5}$ in Shanghai and Beijing, China. Atmos. Environ. 36 (26), 4223–4234.